# Numerical Simulation of Noise from Supersonic Jets Passing Through a Rigid Duct

Max Kandula*
*Sierra Lobo, Inc. (USTDC), Kennedy Space Center, FL 32953*

**The generation, propagation and radiation of sound from a perfectly expanded Mach 2.5 cold supersonic jet flowing through an enclosed rigid-walled duct with an upstream J-deflector have been numerically simulated with the aid of OVERFLOW Navier-Stokes CFD code. A one-equation turbulence model is considered. While the near-field sound sources are computed by the CFD code, the far-field sound is evaluated by Kirchhoff surface integral formulation. Predictions of the farfield directivity of the OASPL (Overall Sound Pressure Level) agree satisfactorily with the experimental data previously reported by the author. Calculations also suggest that there is significant entrainment of air into the duct, with the mass flow rate of entrained air being about three times the jet exit mass flow rate.**

## Nomenclature

| | | |
|---|---|---|
| $c$ | = | sound velocity |
| $d_j$ | = | jet exit diameter |
| $f$ | = | frequency |
| $\dot{m}$ | = | mass flow rate |
| $M$ | = | Mach number, $u/c$ |
| $p$ | = | pressure |
| $p'$ | = | acoustic pressure disturbance |
| $r$ | = | distance from the sound source |
| Re | = | Reynolds number, $\rho_j u_j d_j / \mu_j$ |
| $St$ | = | pressure |
| $T$ | = | temperature |
| $u$ | = | velocity |
| $x, y, z$ | = | Cartesian coordinates |

***GREEK SYMBOLS***

| | | |
|---|---|---|
| $\mu$ | = | dynamic viscosity |
| $\rho$ | = | density |

***SUBSCRIPTS***

| | | |
|---|---|---|
| $j$ | = | jet |
| $\infty$ | = | ambient fluid |

## I. Introduction

The overall process of sound emission from partially ducted rocket exhausts is of great practical interest in the understanding of sound suppression systems for launch vehicles. Clean (dry) launch pads with ducted exhausts

* Sr. Principal Investigator, Associate Fellow AIAA.

are preferable to those fitted with water deluge systems for sound suppression with regard to maintenance costs and the frequency of launches. A detailed knowledge of the behavior of the sound radiation from these ducted exhausts is useful in the design and optimization of the sound suppression systems.

The totality of the far field sound from ducted exhausts is composed of the transmission of sound from the free supersonic jet (upstream of the duct inlet) to the far field, transmission of sound within the duct, and radiation of sound from the duct exit and the subsonic jet (exiting the duct) to the far field. Recent experiments on enclosed duct by Kandula et al.[1-3] have indicated that the jet confinement has a significant effect on sound emission and directivity, suggesting that the duct is modifying the sound generation and propagation. According to Lighthill[4-5], turbulent mixing is responsible for sound generation in jets, with Mach wave radiation (Fflowcs Williams[6]; Tam[7]) manifesting itself in supersonic turbulent jets due to supersonic convection of large scale eddies relative to the ambient.

A number of studies were reported on enclosed subsonic flows typical of turbofan engine inlet/exhaust ducts (for example, Eversman & Roy[8]; Ozyoruk & Long[9]). However, many of the theoretical studies on sound emission from turbulent supersonic jets are focused on unconfined (free) jets (Freund et al.[10]; Gamet & Estivalezes[11]; Kandula & Caimi[12]). The present study is concerned with a theoretical simulation of the effect of the enclosing duct on the radiated noise from cold supersonic jets. Predictions of sound power levels will be compared to the experimental data[1-3].

## I. Computational Simulation

### A. Geometry and Experimental Data

Fig. 1 shows the geometry of the jet-duct configuration considered in the experimental data of Refs. 1-3. The origin of the coordinate system lies in the ground plane, with the $y$-axis coinciding with the jet axis. The jet impinges vertically on an upstream J-deflector (30 deg. to the vertical) of the duct before exiting horizontally through the duct. The nozzle exit diameter is 1 in. The nozzle exit is 73 in. above the ground level, and 10 in. above the duct inlet plane. The duct exit cross section is 6 in. x 12 in. Photographic views of the free jet and the ducted jet testing with Mach 2.5 cold nitrogen jet are displayed in Figs. 2a and Fig. 2b respectively. Fig. 2c shows the sound directivity in the ducted jet system[1-3], with data taken along an 80 in. arc radius about the jet axis, and in a horizontal plane 54 in. above the ground level. In Fig. 2c, the quantity $h$ refers to the height of the nozzle exit plane above the duct inlet plane.

### B. Grid System

A front view of the grid system is presented in Fig. 3a. Fig. 3b shows a representative view of the lateral extent of the grid system. The overall grid system consists of 8 blocks with a total of about $4 \times 10^6$ grid points. Individual grids for the jet, duct, etc., are generated using GRIDGEN grid generation program. The inter-grid communication is established by the Pegasus Code (Benek et al.[13]).

### C. Flow Parameters

The Mach number of the exhaust jet is 2.5, and the jet Reynolds number is 58,300. The jet is perfectly expanded (nozzle exit pressure equals the ambient pressure $p_\infty$ of 14.7 psia). The exit static temperature of the jet is 222 R, indicating that it is a cold jet. The ambient temperature is 530 R.

### D. Solution Procedure

The nearfield solution for the mean flowfield and the acoustic field is obtained by the OVERFLOW CFD Navier-Stokes code (Kandula & Buning[14]). A one-equation turbulence model of Spalart-Allmaras[15] is employed, which solves for the turbulent kinetic energy. Multi-gridding scheme is chosen for accelerated convergence. Initially the steady hydrodynamic flowfield is obtained by running the code with time-stepping. Steady state is achieved in about 2000 iterations. Starting from the steady state solution, a three-dimensional periodic disturbance is applied at the nozzle exit. The disturbance frequency is based on a Strouhal number $St$ =0.2. Thomson's outflow acoustic boundary condition (Thompson[16]) and radiation boundary condition of Tam and Webb[17] are considered. The code is run for about 22000 iterations to ensure that a periodic state is approached.

In the far field, the sound pressure levels are determined by Kirchhoff formulation (Kirchhoff[18] with data on the Kirchhoff surface obtained by the CFD code. The method is presented in Lyrintzis & Mankbadi[19], and has been recently considered by the author for an axisymmetric supersonic jet simulation (Kandula and Caimi[12]). The data on the Kirchhoff surface includes time history of pressure, normal pressure derivative, and pressure-time derivative.

## II. Results

### A. CFD/Kirchhoff Solution

1. *Air Entrainment*

Calculations show that there is significant entrainment of air into the duct. Fig. 4 displays the convergence history of the duct exit mass flow rate until steady state is established. It is seen that the entrained air flow is about 3.2 times the mass flow rate of jet exit. This result is representative of entrainment in practical exhaust duct configurations.

2. *Instananeous Flowfield*

Fig. 5 displays the instantaneous mach number contours in the duct and in the region downstream of the duct exit at a lateral location near the axis of the duct. While the jet exit Mach number is 2.5, the Mach number of flow at the duct exit is subsonic around Mach 0.45.

3. *Acoustic Presssure*

The acoustic pressure (obtained by subtracting the mean pressure from the instantaneous pressure) for the jet-duct system is illustrated in Fig. 6a. The directivity of Mach wave radiation from the initially supersonic jet (unenclosed portion) is observed. The plot also shows the diffraction pattern of sound around the duct. Fig. 6b shows an expanded view of the acoustic pressures within the duct, showing the character of sound reflections and propagation within the duct. It also reveals the acoustic pressure contours in the jet, showing the three-dimensional character of the disturbance in the jet. Calculations show that the OASPL at the location of the jet impingement within the duct is of the order of about 180 dB. Fig. 6c exhibits the acoustic pressure in a near lateral view, showing the near-spherical spreading of the subsonic exhaust from the duct.

### B. Comparison with Experimental Data

The acoustic far field computations of sound levels are based on Kirchhoff surface integral. Fig. 7 presents a comparison of the predictions of the directivity of the OASPL with the test data[1-3] for a closed duct. The OASPL data are presented as a function of the azimuthal angle measured from the axis normal to the duct exit plane. While the free jet data for the OASPL shows symmetry, the OAPSL for the closed duct shows considerable directivity, with the OASPL decreasing with the increasing angle. Satisfactory agreement is noted between the theory and the data. The theory predicts the OASPL with an accuracy of about 2 dB. The results and comparisons will be useful in the development of scaling laws for ducted jet noise, such as those considered for free jets (Kandula and Vu[20]).

## III. Conclusion

Numerical simulation of sound from a supersonic jet passing through a rigid duct with a J-deflector has been carried out. The results provide details of the sound radiation from the free jet and the acoustic field within the duct. The presence of the duct significantly modifies the character of the far-field directivity. Significant level of entrainment of air into the duct has been noted.


## Acknowledgments

This work is partially supported by funding from The Center Director Discretionary Fund (CDDF) at NASA Kennedy Space Center, with Dr. Bruce Vu as technical monitor. Helpful discussions with Dr. Vu are appreciated. Financial support from Maria Littlefield of the ELV directorate at KSC for an 8-processor SGI machine is gratefully acknowledged. Thanks are also due to Prof. Tasos Lyrintzis of Purdue University for kindly providing the YORICK Kirchhoff code.


## References


[1]Kandula, M., and Vu, B., Scale model experiments on sound propagation from a Mach 2.5 cold nitrogen jet flowing through a rigid-walled duct with a J-deflector, NASA TM-2003-211186, Kennedy Space Center, April 2003.

[2]Kandula, M., Margasahayam, R., and Vu, B., Sound propagation from a supersonic jet flowing through a rigid-walled duct with a J-deflector, Proceedings of the 10th International Congress on Sound and Vibration, Stockholm, Sweden, Vol. 4, 2003, pp. 2253-2260.

[3]Vu, B., and Kandula, M., Noise mitigation of ducted supersonic jets for launch exhaust management systems, JANNAF 27th Plume Technology Subcommittee Meeting, NASA Stennis Space Center, Bay St. Louis, Mississippi, May 2003.

[4]Lighthill, M.J., On sound generated aerodynamically, I. General theory, Proc. Roy. Soc. A, 211, 1952, pp. 564-587.

[5]Lighthill, M.J., On sound generated aerodynamically, II. Turbulence as a source of sound, Proc. Roy. Soc. A, 222, 1954, pp. 1-32.

[6]Ffowcs Williams, J.E., The noise from turbulence convected at high speed, Proc. Roy. Soc. A, 255, 1963, p. 469.

[7]Tam, C.K.W., On the noise of a nearly ideally expanded supersonic jet, J. of Fluid Mechanics, Vol. 51, Part I, 1972, pp. 69-95.

[8]Eversman, W., and Roy, I.D., Ducted fan acoustic radiation including the effects of nonuniform mean flow and acoustic treatment, AIAA-93-4424, October 1993.

[9] Ozyoruk, Y., and Long, L., Computation of sound radiated from engine inlets, *AIAA Journal*, Vol. 34, No. 5, May 1996, pp. 894-901.

[10]Freund, J.B., Lele, S.K., and Moin, P., Numerical simulation of a Mach 1.92 turbulent jet and sound field, AIAA J., Vol. 38, No. 11, November 2000.

[11]Gamet, L., and Estivalezes, J.L., Application of large-eddy simulations and Kirchhoff method to jet noise prediction, *AIAA Journal*, Vol. 36, No. 12, December 1998, pp. 2170-2178.

[12]Kandula, M., and Caimi, R., Simulation of jet noise with OVERFLOW CFD code and Kirchhoff surface integral, AIAA-2002-2602, 8th AIAA/CEAS Aeroacoustics conference, June 2002.

[13]Benek, J.A., Buning, P.G., and Steger, J.L., A 3-D grid embedding technique, AIAA-85-1523-CP, July 1985.

[14]Kandula, M., and Buning, P.G., Implementation of LU-SGS algorithm and Roe upwinding scheme in OVERFLOW thin-layer Navier-Stokes code, AIAA-94-2357, June 1994.

[15]Spalart, P.R., and Allmaras, S.R., A one-equation turbulence model for aerodynamic flows, AIAA-92-0439, 1992.

[16]Thompson, K.W., Time-dependent boundary conditions for hyperbolic systems I, *Journal of Computational Physics*, Vol. 89, 1990, pp. 439-461.

[17]Tam, C.K.W., and Webb, J.C., Dispersion relation-preserving finite difference schemes for computational aeroacoustics, *Journal of Computational Physics*, Vol. 107, 1993, pp. 262-281.

[18]Kirchhoff, G.R., Zur Theorie der Lichtstrahlen, *Annalen der Physik und Chermie*, Vol. 18, 1883, pp. 663-695.

[19]Lyrintzis, A.S,. and Mankbadi, R.R., Prediction of the far-field jet noise using Kirchhoff's formulation, *AIAA Journal*, Vol. 32, No. 2, Feb. 1996, pp. 413-416.

[20]Kandula, M., and Vu, B., On the scaling laws for jet noise in subsonic and supersonic flow, AIAA-2003-3288, *9th AIAA Aeroacoustics Conference*, Hilton Head, South Carolina, May 12-14, 2003.

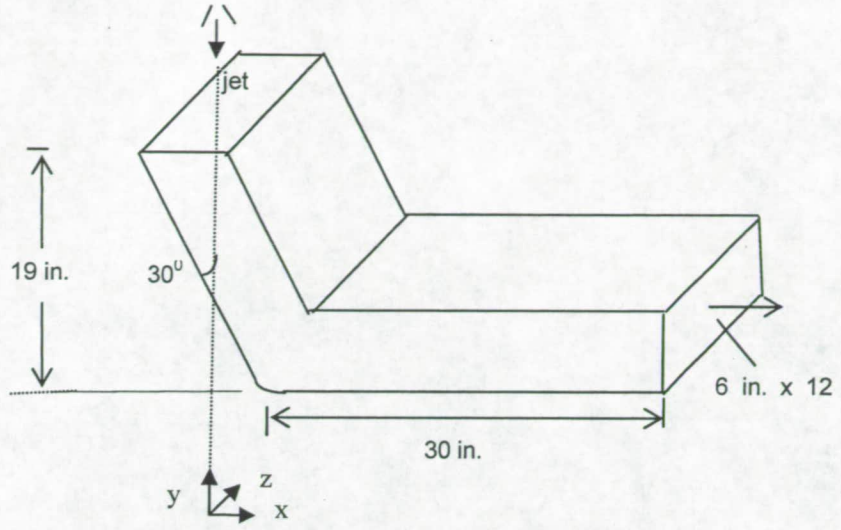


Fig. 1 Geometry of the ducted exhaust jet configuration.

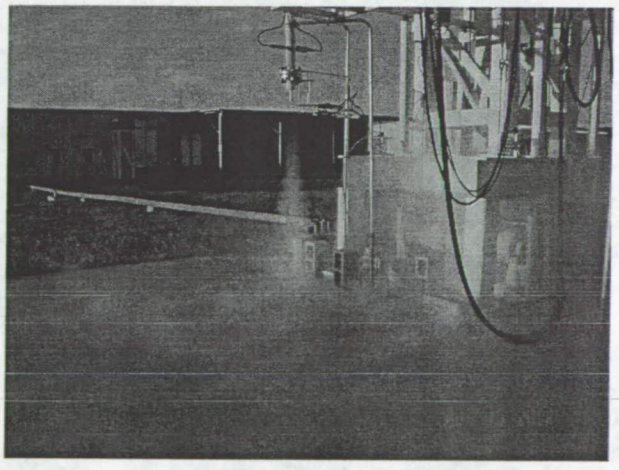

Fig. 2a. Photograph of the nitrogen supersonic free jet.

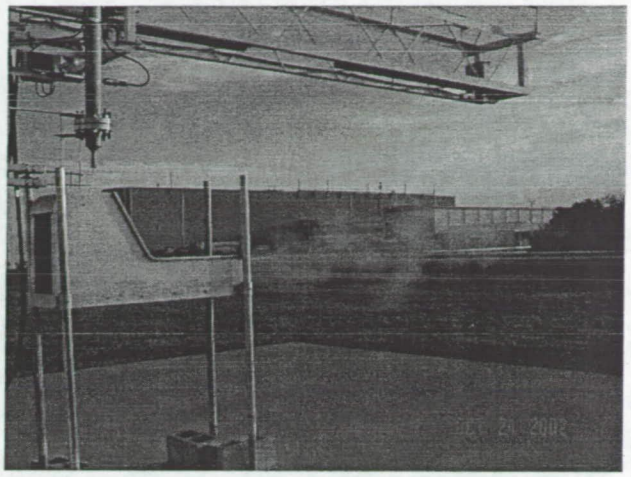

Fig. 2b. Photograph of the nitrogen supersonic jet flowing through an enclosed duct.

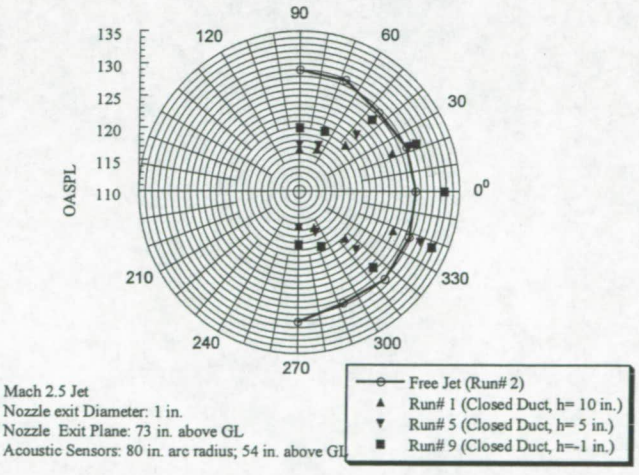


Fig. 2c Effect of nozzle height on the directivity of sound radiation for a closed duct.

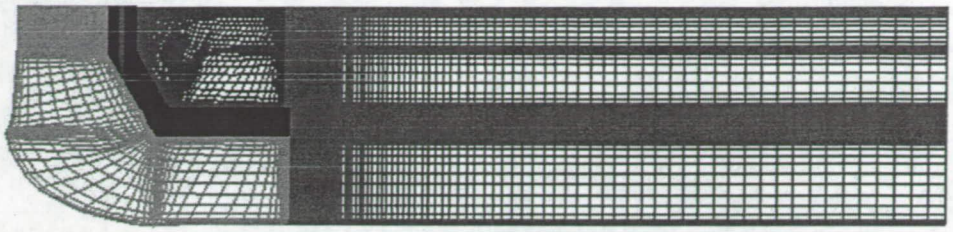

Fig. 3a Grid system for the exhaust (side view).

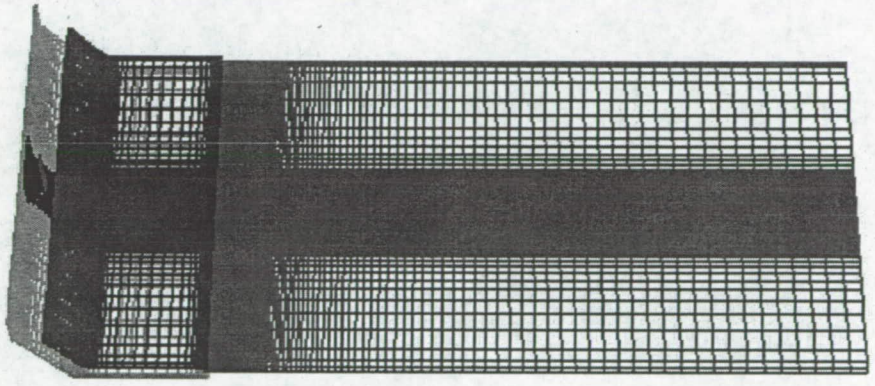

Fig. 3b Grid system for the exhaust (lateral view).

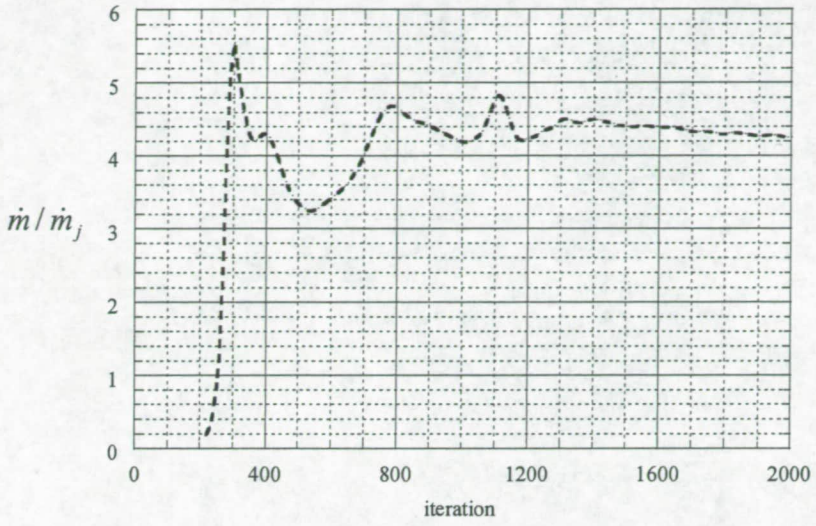


Fig. 4 Convergence history of the duct exit mass flow rate.

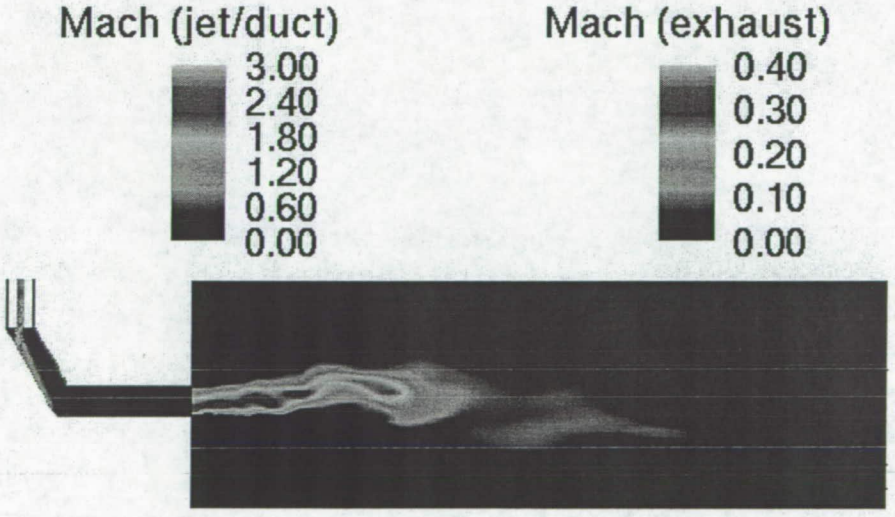


Fig. 5 Instantaneous Mach number contours in the exhaust jet.

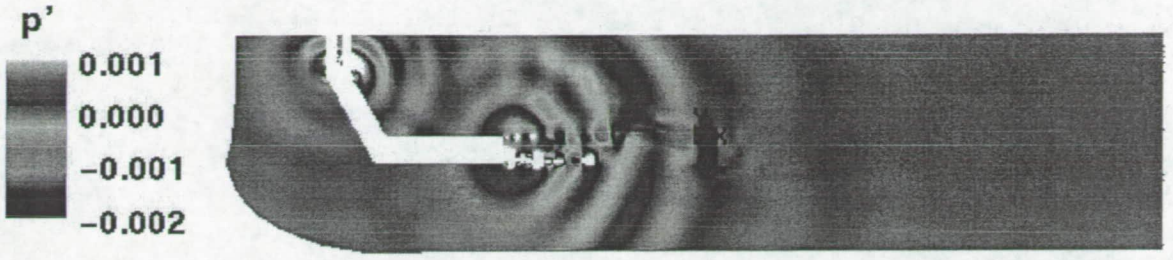


Fig. 6a Acoustic pressure contours in the jet-duct system (excluding the duct).

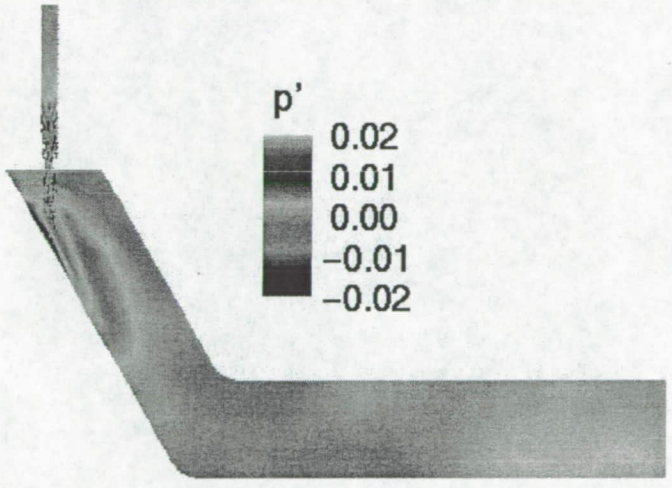


Fig. 6b Acoustic pressure contours in the duct region.

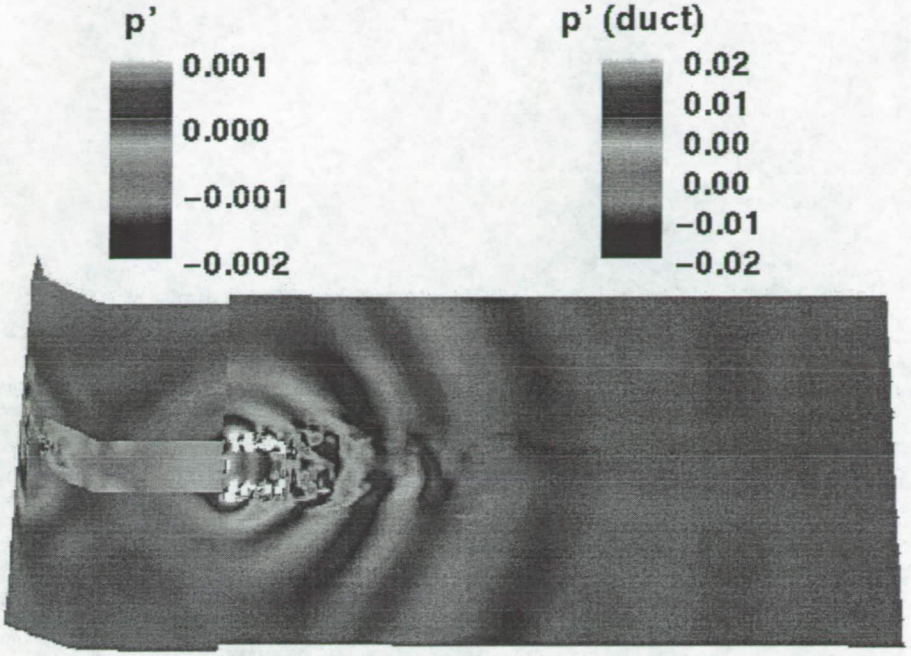


Fig. 6c Acoustic pressure in the lateral view (including the duct).

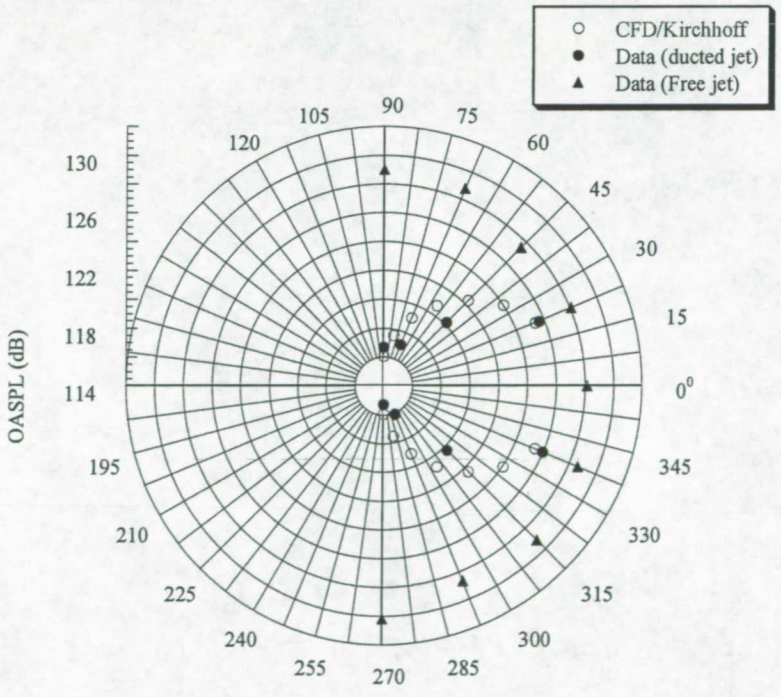


Fig. 7 Comparison of the directivity of Overall Sound Pressure Level.